CO-Induced Segregation of Hydrogen into the Subsurface on Ni(110)

Ali R. Alemozafar and Robert J. Madix*

Department of Chemical Engineering, Stanford University, Stanford, California 94305-5025

Received: October 31, 2003

Scanning tunneling microscopy measurements on Ni(110) suggest that the segregation of hydrogen into the subsurface (β_3) state is mediated by CO. At 375 and 390 K exposure of the saturated added row Ni−H overlayer to 1×10^{-8} Torr of CO(g) induces the dissolution of the Ni−H rows to yield Ni islands of monatomic step height. Structures associated with the adsorption of CO onto the clean surface are not observed, and the surface formed under these conditions is resistant toward hydrogen uptake upon further H_2(g) exposure. This reconstruction is activated; it does not occur at temperatures below 370 K at the same pressure of hydrogen. With heating, H_2 is evolved from the β_3 desorption state from this surface; no other gases are observed to desorb. Cooling the surface to room temperature permits formation of the "normal" Ni−H overlayer upon further H_2(g) exposure. These findings suggest that at temperatures above 370 K CO induces a surface reconstruction with a fraction of the hydrogen from the Ni−H overlayer segregating into the subsurface, while the remainder evolves into the gas phase. Under a constant CO background pressure of 6×10^{-8} Torr at 350 K a low-coverage c(4×2)-CO structure appears as unresolved [001]-oriented rows separated by four unit vectors along [1$\bar{1}$0]. The mobility of CO along the [001] azimuth appears to result in a loss of surface registry of CO in that direction.

1. Introduction

Ni is well-known for its applications in hydrogenation catalysts.[1] Over the past 30 years, investigations into the interaction between hydrogen and the Ni(110) surface have yielded a much better understanding of adsorbate to surface interactions. Because the H/Ni(110) interaction is unusual, it warrants further study. On Ni(110) hydrogen and Ni interact at room temperature to form extended [1$\bar{1}$0]-oriented chains of −Ni−H−, separated from one another by two lattice units in the [001] direction:[2]

$$H_2 + 2Ni \rightarrow 2\ -Ni-H- \qquad (1)$$

In this process, Ni is "leached" from terraces and step edges to form "missing" rows oriented along the [1$\bar{1}$0] direction. With increasing coverage lateral interactions between chains affect the two-dimensional condensation of the Ni−H overlayer:[3]

$$-Ni-H- \rightarrow Ni-H\ (\text{overlayer}) \qquad (2)$$

This surface state displays a streaky (1×2) low-energy electron diffraction (LEED) pattern. Upon heating, hydrogen desorbs from the surface at approximately 350 K (β_2 desorption state) (Figure 1a).[4] In this process the Ni atoms in the Ni−H overlayer are liberated to return to step edges, refill missing rows, or crystallize into islands of monatomic step height. Furthermore, Norton and Harrington have shown that when the surface is cooled in D_2(g) from temperatures greater than 350 K, a third desorption state (β_3) with a desorption peak centered at approximately 435 K appears and saturates at 0.06 monolayer (ML). The lack of a change in the surface work function during desorption of this state (Figure 1a), which is also consistent with work-function measurements by Chrstmann et al.,[4] led the authors to suggest that hydrogen evolves from sites beneath the surface (i.e., subsurface hydride).[5] Any attempt to increase the coverage of the β_3 state proved unsuccessful, leaving the origin of the relatively small coverage of the state unknown.

Studies of CO adsorption on Ni(110) have utilized an array of surface analytical instruments. With heating, CO is seen to evolve from the surface at 330 K (α_1) and 420 K (α_2) (Figure 1b).[6] LEED studies reveal several equilibrium surface structures with increasing CO coverage, namely, c(8×2)-, c(4×2)-, and p(2×1)-2CO structures, which saturate at 0.63, 0.77, and 1.0 ML, respectively. The final structure has been further studied with scanning tunneling microscopy (STM), where coadsorption measurements with O and S led the investigators to suggest that the CO molecules occupy short-bridge sites and alternately tilt away from the surface normal.[7]

The study of the coadsorption of hydrogen and CO on Ni(110) has been of interest primarily due to the utility of Ni in catalyzing methanation reactions.[8] Work by Küppers and coworkers revealed very complex behavior associated with the coadsorption of hydrogen and CO on Ni(110).[9] The desorption of H_2(g) is affected by the presence of CO and depends on the adsorption sequence. Through LEED, high-resolution electron energy loss spectroscopy (HREELS), and temperature-programmed desorption (TPD) investigations, the authors suggested cooperative adsorption phenomena.

In this paper we present the findings from our STM, TPD, and Auger electron spectroscopy (AES) investigation of the Ni(110)-p(1×2)-H system at temperatures above 350 K. Our findings provide further evidence for the formation of a subsurface hydride state. Exposing a saturated Ni−H overlayer to CO(g) at temperatures above 375 K results in the precipitation of Ni islands. Only H_2 (β_3) desorbs from this surface with heating. This result suggests that CO induces the segregation of a fraction of the hydrogen from the Ni−H overlayer into the subsurface, while the remainder evolves into the gas phase. We have also been able to image the low-coverage c(4×2)-CO structure, which, under a constant 6×10^{-8} Torr CO background

10.1021/jp031208k CCC: $27.50
Published on Web 05/05/2004

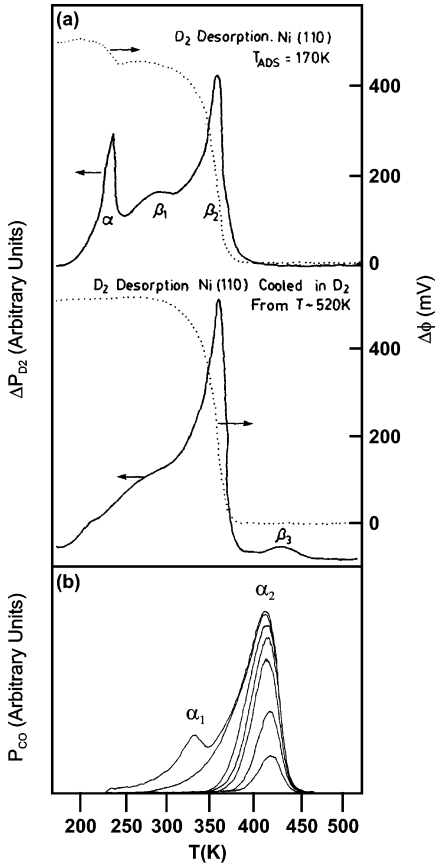

Figure 1. Ni(110) reference spectra, showing (a) TPD and surface work function ($\Delta\phi$) measurements, adapted from ref 5. The plot at the top was obtained following saturation exposures of the clean surface at 170 K to D_2(g), the surface of which exhibited a (1×2) LEED pattern. The bottom plot was obtained after the surface was cooled in $\sim 10^{-4}$ Pa of D_2(g) from 520 to 170 K. (b) TPD spectra after varying exposures of CO to the surface at 130 K, adapted from ref 6.

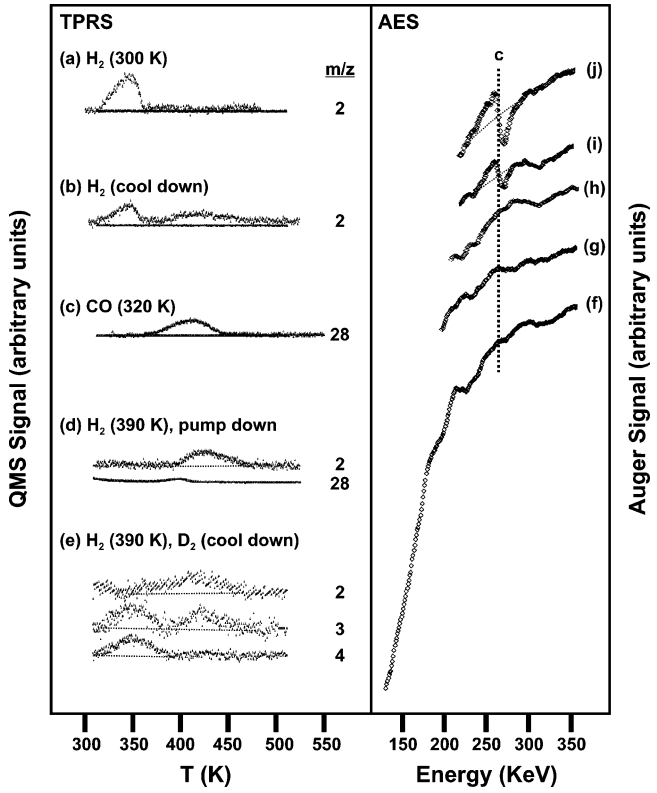

Figure 2. H_2(g) ($m/z = 2$) and/or CO(g) ($m/z = 28$) TPD spectra following (a) H_2(g) adsorption onto the clean surface at 300 K (6×10^{-6} Torr, 5 min), (b) cooldown from 390 to 300 K in 6×10^{-6} Torr of H_2(g), (c) CO(g) adsorption (1×10^{-7} Torr, 10 min) at 320 K, (d) H_2(g) adsorption at 390 K (6×10^{-6} Torr, 5 min), followed by a pumpdown to approximately a 5×10^{-9} Torr background pressure and subsequently a cooldown to room temperature, and (e) H_2(g) exposure at 390 K (6×10^{-6} Torr, 4 min) followed by a pumpdown to approximately a 5×10^{-9} Torr background pressure and then a cooldown to room temperature in 1×10^{-7} Torr of D_2(g). The AES spectra show the composition of (f) the surface following our cleaning procedure and (g) H_2(g) adsorption at 390 K (6×10^{-6} Torr, 5 min), (h) the surface obtained by dosing H_2(g) (1×10^{-6} Torr, 2 min) followed by CO(g) (1×10^{-8} Torr, 2 min) under a steady H_2(g) background and (i) adsorption of 60 L of CO(g) at 312 K and (j) a p(4×5)-C surface, obtained by dosing acetic acid at room temperature and annealing to 600 K.

pressure at 350 K, appears as unresolved [001]-oriented rows separated by four unit vectors along the [1$\bar{1}$0] direction, namely, a p(4×1) structure.

2. Experimental Section

Experiments were performed in an ultrahigh vacuum chamber equipped with a scanning tunneling microscope, a quadrupole mass spectrometer (QMS) used for TPD measurements, LEED optics, and an Auger electron analyzer. The chamber was also equipped with a sputter ion gun and stainless steel gas dosers. The system exhibited a base pressure of 2×10^{-10} Torr (with mainly H_2 and CO in the background) following cleaning of the surface, which rose to approximately 5×10^{-10} Torr during the experiments. A heating rate of 1 K/s was employed for all TPD measurements.

The homemade "Johnnie Walker"-type scanning tunneling microscope utilizes RHK STM 100 control electronics and a Pt/Ir tip. The tip was prepared in a vacuum via field-induced evaporation onto a gold foil (~4 μA, 15 min). STM scan dimensions were calibrated with the Ni(110)-p(2×1)-O structure.[10]

The crystal was aligned to within 0.5° of the (110) plane using Laue backscattering and was mechanically polished with alumina paste down to 0.3 μm. The crystal was cleaned in a vacuum by three cycles of Ar ion sputtering (2 μA, 500 eV, 600 K, 10 min) and annealing (1050 K, 10 min), with the first anneal done in an oxygen atmosphere (1×10^{-7} Torr) to cleanse the surface of impurities observed in STM images. This procedure yielded a clean and ordered surface, as assessed via AES, a sharp p(1×1) LEED pattern, and subsequent high-resolution STM images. The crystal could be cooled to 120 K with liquid nitrogen and heated to 1100 K by electron bombardment to the back of the crystal. The temperature was monitored by a chromel−alumel thermocouple spot-welded to the back of the crystal. The STM ramp housing the crystal and the STM scan head were allowed to thermally equilibrate for 30 min prior to STM measurements.

The purities of H_2(g) (Praxair, 99.8%), D_2(g) (Matheson, 99.7%), CO(g) (Praxair, 99.99%), and O_2(g) ($^{16}O_2$, Praxair, 99.999%) were monitored with the QMS during dosing; all gases were dosed from the background. Coverages were obtained by measuring the fraction of the area occupied by a particular structure and multiplying that value by its local coverage (i.e., 0.5 for the −Ni−H− added rows as the local coverage of the Ni(110)-p(1×2)-H structure is 0.5 ML).

3. Results and Discussion

3.1. TPD and AES Investigations. TPD spectra for H_2 and CO (Figure 2a−e) were obtained at a constant heating rate of

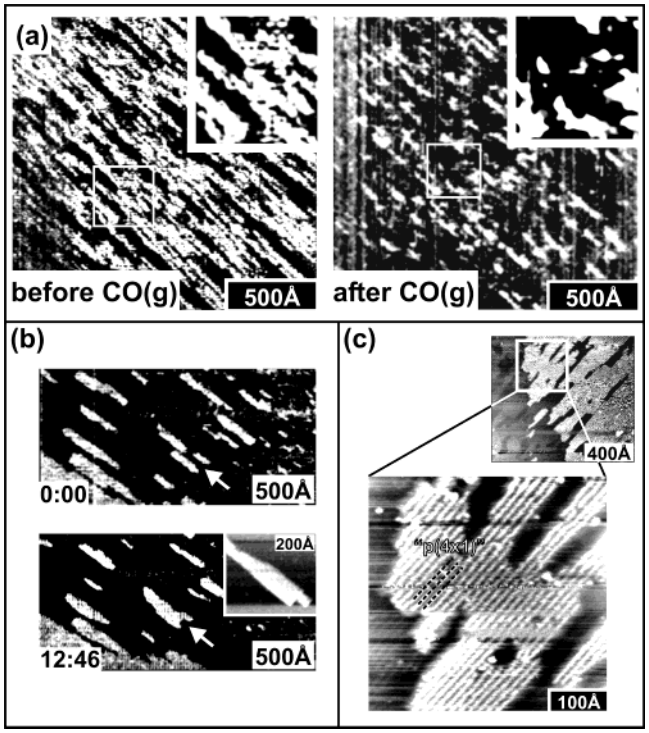

Figure 3. (a) STM images showing changes to the Ni−H-covered surface at 375 K before and after CO(g) exposure (1.0×10^{-8} Torr) at a fixed H_2(g) pressure (1.3×10^{-6} Torr). Tunneling conditions: −97.7 mV, set-point current 0.60 nA (constant height). The insets are contrast-enhanced enlargements of the boxed areas. (b) The plateaus coalesce in time to form larger structures. Tunneling conditions: −97.9 mV, 67.2 pA (0:00 frame, constant height) and −11.4 pA (12:46 frame, constant height). The inset of the 12:46 frame shows a close-up of one of the Ni plateaus. Tunneling conditions: −0.55 V, 250 pA (constant height). (c) p(4×1)-CO reference structure. Tunneling conditions: −226 mV, 319 pA (top frame, constant height) and 322 pA (bottom frame, constant height).

1 K/s. Dosing H_2(g) onto the clean surface at room temperature populates the β_2 desorption state with a peak temperature at 347 K (Figure 2a). Spectra obtained following H_2(g) exposure at 6×10^{-6} Torr during cooldown from 390 K to room temperature (approximately 15 min) reveal the β_2 desorption state and a broad, higher temperature desorption state (β_3) with a peak maximum centered at 425 K (Figure 2b). Following this treatment, CO desorption, which normally takes place at approximately 410 K (Figure 2c), was not observed. A TPD spectrum obtained by dosing H_2(g) at 390 K followed by a pumpdown and subsequent cooldown to 300 K shows hydrogen evolving from the β_3 desorption state only, suggesting that the β_3 state is the result of hydrogen adsorption at temperatures above the β_2 state (Figure 2d), consistent with the conclusions of Norton and Harrington.[5] The lower temperature (β_2) desorption state was not observed, and little CO (0.05 ML) desorbed from the surface. A TPD spectrum of the surface after H_2(g) exposure at 390 K followed by a pumpdown and subsequent cooling (approximately 15 min) to room temperature in a background pressure of 1×10^{-7} Torr of D_2(g) (Figure 2e) shows D_2(g) evolving primarily from the β_2 state and H_2 from the β_3 state. The mixed product, HD, is seen to desorb at both temperatures, which suggests exchange between the two states.

AES was used to clarify the surface composition upon formation of the β_3 state (Figure 2f−j). An AES spectrum obtained following our cleaning procedure (Figure 2f) shows the surface to be devoid of carbon (~272 eV). The spectrum remains nearly the same following exposure of the surface to hydrogen at 390 K (Figure 2g), giving the β_3 desorption state. Reference AES spectra for ~0.8 ML of CO (Figure 2i) and p(4×5)-carbon-covered surfaces (Figure 2j) are shown for comparison. Figure 2h shows an AES spectrum (obtained at 390 K) following dosing of CO(g) (1×10^{-8} Torr for 2 min) onto a Ni−H-overlayer-covered surface (as evidenced by STM) at 390 K. The spectrum shows the surface to be free of any carbon-containing species.

3.2. CO-Induced Subsurface Segregation of Hydrogen. Dosing CO onto a saturated Ni−H overlayer results in the dissolution of the hydrogen structure, suggesting that carbon monoxide induces the segregation of hydrogen to the subsurface (see section 3.3). The clean surface at 375 K was exposed to 1.3×10^{-6} Torr of H_2(g) to adsorb hydrogen on the surface. Growth of the Ni−H structures subsided (i.e., a gas−solid equilibrium was established at 375 K) in about 6 min (Figure 3a, before). CO was introduced to the Ni−H overlayer in the background at 1×10^{-8} Torr with the hydrogen pressure kept constant at 1.3×10^{-6} Torr. This change resulted in the breakup of the Ni−H structure and precipitation of the Ni into anisotropic plateaus of monatomic step height (Figure 3a, after). The resulting state of the surface was resistant to further H_2(g) adsorption, as the Ni−H overlayer did not form regardless of the background hydrogen pressure ($(1-2) \times 10^{-6}$ Torr) or duration of exposure ($t > 30$ min). The CO-induced formation of the Ni-plateau-covered surface occurred after nearly 2 min under the scanning tunneling microscope, presumably due to the tip shielding of the imaging area, which decreases the effective CO exposure by a factor of ~10.[11] In time the Ni plateaus coalesced to form larger structures (Figure 3b, white arrow). A magnification of one of these Ni plateaus (Figure 3b, 12:46 frame, inset) shows it to be devoid of Ni−H rows and either low-coverage (Figure 3c) or high-coverage p(2×1)-CO structures,[3,7] in agreement with the p(1×1) LEED pattern observed. The CO structure shown in Figure 3c was obtained by imaging the clean and uncovered surface at 350 K at a CO-(g) background pressure of 6×10^{-8} Torr. The streaky [001]-oriented rows are separated by four lattice units in the [1$\bar{1}$0] direction, giving a p(4×1) structure, which we interpret as the c(4×2)-CO structure (see the Introduction). This is consistent with the faint c(4×2) LEED pattern obtained for this surface. Mobility of CO in the direction of the [001] vector gives rise to the streakiness in the STM images.

Exposure of the Ni−H-covered surface to 1×10^{-8} Torr of CO at 390 K also induces the breakup of the Ni−H overlayer, Figure 4a. The hydrogen pressure was kept constant at 5×10^{-6} Torr during CO exposure. The temperature of 390 K is at the leading edge of the CO desorption peak centered at 410 K (Figure 2c). No CO structures (Figure 3c) were observed on the surface. This outcome is identical to what was observed at 375 K (Figure 3a). An expanded view of the surface (Figure 4b) shows a distribution of Ni islands with a number density that increases with distance from the steps. The coverage of Ni plateaus at locations far from a step edge is approximately 0.14 ML. Structures expected for adsorbed hydrogen or CO were not observed on either the terraces or islands following the sequence of images. A separate TPD measurement (Figure 4c) shows occupancy of the β_3 state, as H_2(g) is seen to desorb at approximately 425 K. The surface prepared at 390 K under the conditions employed during the STM measurements was cooled to 375 K (5 min) prior to the TPD measurement. Cooling took approximately 2 min. CO was not seen to desorb from this surface. This result is significant since kinetic calculations predict a steady-state CO coverage of approximately 0.4 ML

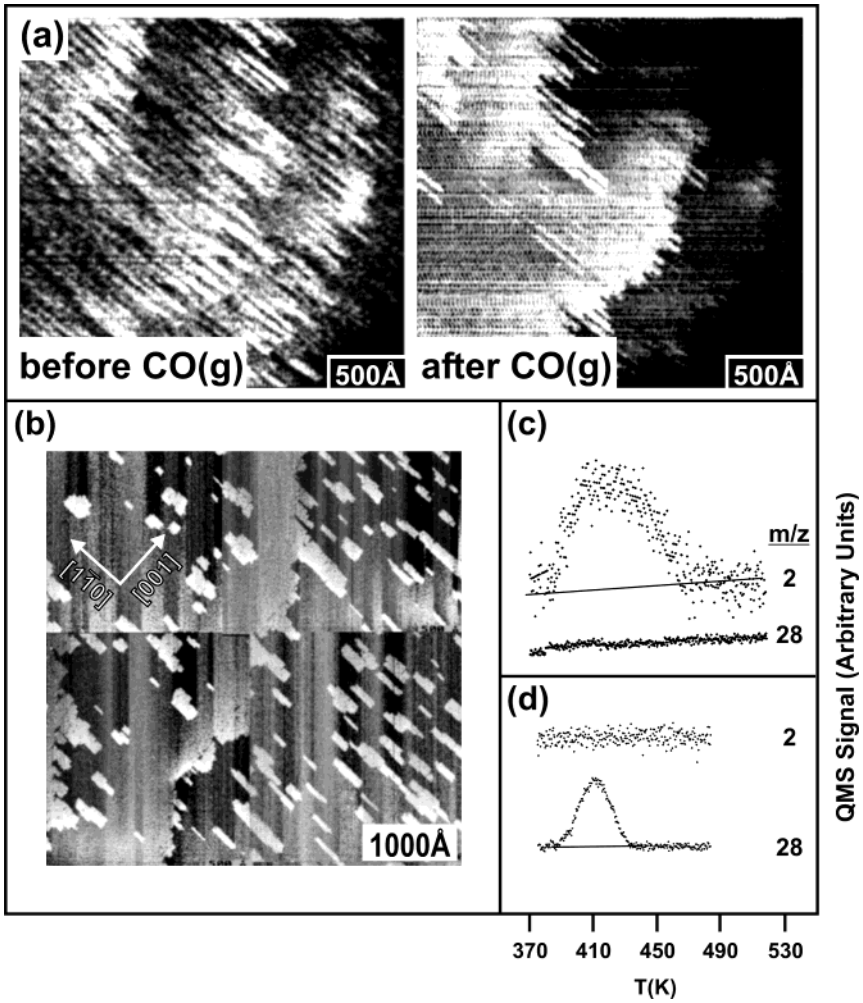

Figure 4. (a) STM image showing changes to the Ni−H overlayer at 390 K before and after CO(g) exposure (1×10^{-8} Torr) at a fixed H_2(g) pressure (5×10^{-6} Torr). Tunneling conditions: −98.5 mV, set-point current 0.60 nA (constant height). The Ni−H overlayer was obtained via H_2(g) exposure for 5 min at 5×10^{-6} Torr. (b) An expanded view of the surface following the sequence in (a). Tunneling conditions: −98.7 mV, set-point current 0.60 nA (constant height). (c) TPD spectra of the surface in (a) following cooldown to 375 K. (d) TPD spectra following exposure of the clean surface to CO(g) at 390 K and cooldown to 375 K.

on clean Ni(110) under these experimental conditions. A blank TPD measurement with CO(g) dosed onto the clean surface at 390 K (1×10^{-7} Torr, 3 min) followed by a rapid cooldown (2 min) to 375 K shows the desorption of CO with a peak temperature centered at 410 K (Figure 4d).

Cooling the surface in Figure 4b to room temperature in a background pressure of 3×10^{-8} Torr of H_2(g) does regenerate the Ni−H overlayer (Figure 5). This behavior is in agreement with the normal adsorption of hydrogen onto the surface to form −Ni−H− chains and, eventually, the Ni−H overlayer. A zoomed-in view of the surface (Figure 5b) reveals moieties comprising the Ni−H overlayer, the dimensions of which correspond to −Ni−H− double chains.[3,12] TPD measurements of this surface show both the β_2 and β_3 desorption states, indicative of hydrogen evolving from both surface and subsurface sites.

3.3. Subsurface Segregation Phenomenon. The most logical explanation for the dissolution of the hydrogen overlayer (Figures 3 and 4) is the segregation of hydrogen from the Ni−H structure into the subsurface. STM measurements showed none of the known structures associated with the adsorption of hydrogen upon formation of the β_3 state, which suggests that, with heating, hydrogen in the β_3 state evolves from either a surface state that cannot be imaged by the STM or subsurface sites. Cooling this surface to room temperature permits the normal development of the Ni−H overlayer upon further hydrogen exposure; TPD measurements of the surface prepared in this manner showed hydrogen evolving from both the β_2 and β_3 desorption states. The β_2 desorption peak has been attributed to hydrogen from the Ni−H overlayer.

CO-induced subsurface segregation of hydrogen is the result of close interplay between CO−Ni and H−Ni. The overall process, namely, the segregation of H to the subsurface, can be represented by a series of transient elementary steps, shown schematically in Figure 6:

$$\mathrm{CO(g) + Ni{-}H \rightarrow CO{-}Ni{-}H} \qquad \text{(coadsorption)} \quad (4)$$

$$\mathrm{CO{-}Ni{-}H \rightarrow CO{-}Ni{-}H{-}Ni(second\ layer)} \qquad \text{(displacement)} \quad (5)$$

$$\mathrm{CO{-}Ni{-}H{-}Ni(second\ layer) \rightarrow CO(g) + Ni(plateaus) + Ni(second\ layer){-}H} \qquad \text{(CO desorption)} \quad (6)$$

The transient interaction between CO and Ni in the Ni−H overlayer sufficiently perturbs the Ni−H bond to affect the segregation of a fraction of H to the subsurface to yield a species of the form Ni(second layer)−H (eq 6). This subsurface H appears, in turn, to weaken the bonding of both CO and H to

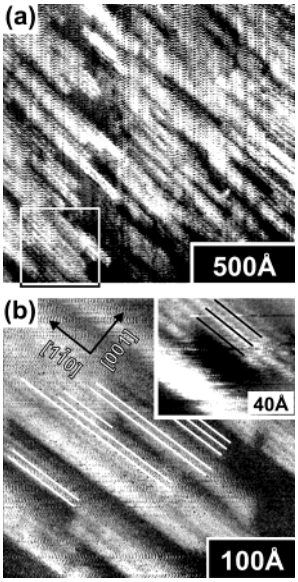

Figure 5. (a, top image) STM image of the surface in Figure 4b following cooldown to room temperature in 3×10^{-8} Torr of H_2(g). Tunneling conditions: −190 mV, set-point current 0.60 nA (constant height). (b, bottom two images) Magnifications of the boxed area in (a). The p(1×2)-H rows are better resolved in the inset. White lines have been added to accentuate the contrast for the purposes of publication.

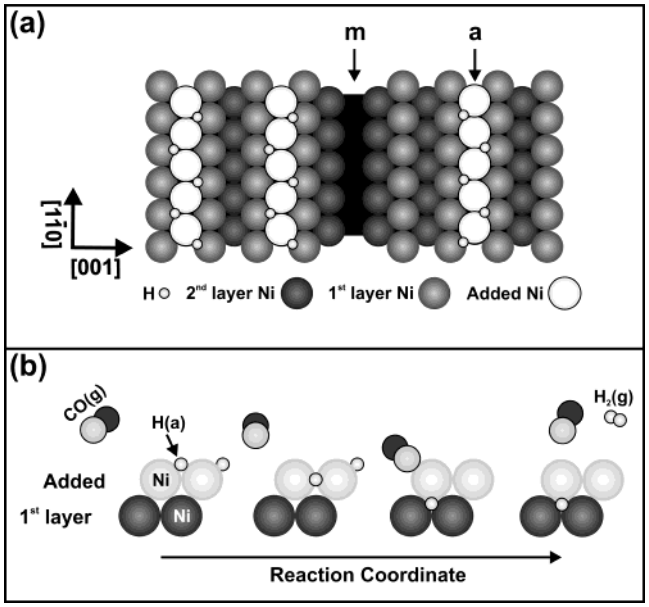

Figure 6. Two-dimensional model of (a) the Ni−H structure, showing the p(1×2)-H added (a) and missing rows (m). (b) A series of events that suggest the process by which CO induces the segregation of atomic hydrogen to the subsurface.

the outer surface. From the saturation coverage of subsurface hydrogen (0.06 ML; see the Introduction) and the initial Ni−H overlayer coverage (0.13 ML), the segregation of hydrogen into the subsurface is concomitant with the evolution of approximately 0.07 ML of H_2(g). The recombination of hydrogen adatoms to yield H_2(g) may be due to the destabilization of the Ni−H overlayer.

The CO-induced segregation of hydrogen to the subsurface was not observed at lower temperatures (below 370 K), suggesting that it is an activated process. For example, the dissolution of the Ni−H overlayer observed at 390 K and a 6×10^{-6} Torr background H_2(g) pressure (Figure 4a) was not observed at 360 K.[3] This observation is consistent with the work by Harrington and Norton, in which the β_3 state was obtained by exposing the surface to deuterium at high temperatures (during cooldown).

Adsorbate-induced segregation to the subsurface has been observed previously, particularly in studies involving the adsorption of oxygen onto a transition-metal alloy surface. Nakanishi et al. have seen that, upon oxygen adsorption, Au in the topmost layer of $Au_3Cu(001)$ was replaced by Cu, and Cu in the second layer by Au.[13] This effect is due to the Cu−O bond being stronger than the Au−O bond. Surface segregation behavior was further corroborated theoretically by Poon and co-workers, who showed that the Au_3Cu alloy, which initially has a Au-rich top layer and a Cu-rich second layer, becomes Cu-rich in the presence of a monolayer of oxygen.[14] Finally, a study with the chemisorption of oxygen on Au−Ag vacuum-deposited alloy films has shown oxygen to induce changes to the I−E profiles during the initial potential scans, leading Lazarescu et al. to suggest the oxygen-induced segregation of Ag into the bulk.[15]

Subsurface hydrogen has been identified on the Ni(111) and Cu(110) surfaces. On Ni(111), Ceyer et al. used TPD measurements to show that a surface obtained via exposure to hydrogen atoms exhibits over 8 MLs of hydrogen desorbing from the subsurface with temperature.[16] Rieder and Stocker used LEED and He diffraction techniques to reveal a subsurface reconstructed (1×2)-H phase on Cu(110), the structure of which extends to the surface at higher H coverages.[17]

4. Summary

We have combined STM with TPD and AES to show changes to the Ni(110) surface structure upon formation of the β_3 state of hydrogen, which has been ascribed to subsurface hydrogen. At 375 and 390 K exposure of the saturated Ni−H added row overlayer to CO induces dissolution of the hydrogen structures to yield anisotropic plateaus of Ni. The surface prepared in this manner is resistant toward further H_2(g) exposure. Neither H_2 nor CO adsorption was observed on the surface at these temperatures. In this step, a fraction of the H from the Ni−H overlayer goes subsurface while the remainder evolves as H_2(g). The segregation of H to the subsurface is due to the close interplay between CO and Ni−H. On Ni(111) subsurface hydrogen has been shown to be more reactive than its surface-adsorbed counterpart particularly with respect to the hydrogenation of electronically unsaturated systems such as ethylene and acetylene.[16] The reactivity of subsurface hydrogen on Ni(110) with similar molecules awaits further investigation.

We have imaged the low-coverage c(4×2)-CO structure, which, under a constant 6×10^{-8} Torr CO background pressure at 350 K, appears as unresolved [001]-oriented rows separated by four unit vectors along [1$\bar{1}$0], namely, a p(4×1) structure. It is suggested that the mobility of CO along [001] results in a loss of surface registry of the c(4×2) structure in the direction of the [001] vector.

Acknowledgment. We thank the National Science Foundation (Grant NSF CHE 9820703) for support of this work.

References and Notes

(1) Christmann, K. *Bull. Soc. Chim. Fr.* **1985**, *3*, 288.
(2) Nielsen, L. P.; Besenbacher, F.; Laegsgaard, E.; Stensgaard, I. *Phys. Rev. B* **1991**, *44*, 13156.
(3) Alemozafar, A. R.; Madix, R. J. Manuscript in preparation.
(4) Christmann, K.; Schober, O.; Ertl, G.; Neumann, M. *J. Chem. Phys.* **1974**, *60*, 4528.
(5) Harrington, D. A.; Norton, P. R. *Surf. Sci.* **1988**, *195*, L135.

(6) Behm, R. J.; Ertl, G.; Penka, V. *Surf. Sci.* **1985**, *160*, 387.
(7) Sprunger, P.; Besenbacher, F.; Stensgaard, I. *Surf. Sci.* **1995**, *324*, L321.
(8) Guo, X.-C.; King, D. A. Coadsorption of Carbon Monoxide and Hydrogen on Metal Surfaces. In *The Chemical Physics of Solid Surfaces*; King, D. A., Woodruff, D. P., Eds.; Elsevier: Amsterdam−London−New York−Tokyo, 1993; p 113.
(9) Bauhofer, J.; Hock, M.; Küppers, J. *J. Electron Spectrosc. Relat. Phenom.* **1987**, *44*, 55.
(10) Eierdal, L.; Besenbacher, F.; Lægsgaard, E.; Stensgaard, I. *Surf. Sci.* **1994**, *312*, 31.
(11) Besenbacher, F.; Norskov, J. K. *Prog. Surf. Sci.* **1993**, *44*, 5.
(12) Grigo, A.; Badt, D.; Wengelnik, H.; Neddermeyer, H. *Surf. Sci.* **1994**, *331−333*, 1077.
(13) Nakanishi, S.; Kawamoto, K.; Fukuoka, N.; Umezawa, K. *Surf. Sci.* **1991**, *261*, 342.
(14) Poon, H. C.; Khanra, B. C.; King, T. S. *Phys. Rev. B* **1993**, *47*, 16494.
(15) Lazarescu, V.; Radovici, O.; Vass, M. *App. Surf. Sci.* **1992**, *55*, 297.
(16) Ceyer, S. T. *Acc. Chem. Res.* **2001**, *34*, 737.
(17) Rieder, K. H.; Stocker, W. *Phys. Rev. Lett.* **1986**, *57*, 2548.